

Crystal Growth and Electro-optical Characterization of $\text{In}_2\text{Se}_{2.7}\text{Sb}_{0.3}$ Compound

Piyush Patel^{1,*}, S.M. Vyas^{2,†}, Vimal Patel², Himanshu Pavagadhi²

¹ Department of Physics, Khyati Institute of Science, Khyati Foundation, Gujarat, India

² Department of Physics, School of Sciences, Gujarat University, Ahmedabad, 380009 Gujarat, India

(Received 08 February 2020; revised manuscript received 15 August 2020; published online 25 August 2020)

The III-VI group of semiconducting materials is mostly used for the developing of ionizing radiation detectors, solid-state electrodes as well as solar cell, photosensitive heterostructures and ionic batteries. Layer structure of III-VI semiconductor crystals have been extensively studied as a two-dimensional crystal system. In_2Se_3 semiconductor with A_2B_3 general compound formula has a hexagonal crystal structure. $\text{In}_2\text{Se}_{2.7}\text{Sb}_{0.3}$ has been grown by the Bridgman technique. The freezing interference temperature gradient was 60 °C/cm and the best quality crystals have been obtained at a growth velocity of 0.35 cm/h. The crystal perfection was studied under optical microscope, with a various growth feature observed on top free surface of the crystal which is predominant of layer growth mechanism. EDAX technique has been used for testing the presence of constituent elements of $\text{In}_2\text{Se}_{2.7}\text{Sb}_{0.3}$ compound. Defect formation in crystals is a key event making growth possible under near-equilibrium conditions. In this work, the morphological study was performed by atomic force microscopy of the surface of the crystal compound. The temperature dependence of electrical resistivity of $\text{In}_2\text{Se}_{2.7}\text{Sb}_{0.3}$ compound was studied using four-probe technique. The band gap was determined using UV-Vis spectrophotometer in the wavelength range 200 nm to 900 nm. From these characterizations the results and conclusions are reported in this paper.

Keywords: Surface features, Layer growth, Bridgman technique, Resistivity, Optical band gap.

DOI: [10.21272/jnep.12\(4\).04022](https://doi.org/10.21272/jnep.12(4).04022)

PACS numbers: 81.10. – h, 72.20. – i, 78.20. – e

1. INTRODUCTION

In_2Se_3 is the most extensively studied because of its potential application in photovoltaic devices. J. Jasinski et al. [1] worked on the crystal structure of In_2Se_3 with k -phase due to its application. They investigated the crystal structure of In_2Se_3 with single phases k and γ as well as found the lattice parameters for both. They compared the both parameters and observed that the k -phase has larger unit cell compared to the γ -phase and the structure is more similar to γ -phase.

From the survey, In_2Se_3 has a high absorption coefficient as well as energy band gap in the range that is optimal for solar energy conversion. For that, Hee Moon Oh et al. [2] studied the growth and characterization of In_2Se_3 of α -phase and they used the chemical transport reaction technique for the crystal growth. In the characterization of In_2Se_3 , they found that its energy band gap at 298 K is 1.42 eV for direct transition.

The ternary semiconductor compounds in either single crystal or thin film form have received considerable interest because of their structural, optical and electrical properties which allow their wide use in many electronic and optoelectronic devices [3, 4].

Michel Spiesser et al. [5] studied the preparation and properties of two indium antimony selenides. They used the Bridgman technique for the crystal growth and studied the optical properties carried out for $\text{In}_{1.8}\text{Sb}_{0.2}\text{Se}_3$, which is an n -type semiconductor with a band gap of 1.1 eV, and for InSbSe_3 , which is a p -type semiconductor with a band gap of 0.92 eV.

In the present paper, $\text{In}_2\text{Se}_{2.7}\text{Sb}_{0.3}$ crystal was grown by the Bridgman method. We report here the crystal growth features observed on the top free surface of the

as-grown crystal. The electrical resistivity was measured in the temperature range 303 K to 393 K using four-probe technique, and the Hall measurements were carried out at room temperature using Ecopia Hall effect measurement system (HMS-3000). The optical band gap was measured using UV-Vis spectrophotometer.

2. EXPERIMENTAL TECHNIQUE

5N purity In, Bi and Se metals were used for the growing of $\text{In}_2\text{Se}_{2.7}\text{Sb}_{0.3}$ compound. They were weighted into stoichiometric proportion and sealed into a quartz tube with vacuum of the order of 10^{-5} torr. Charge-containing quartz tube was placed into an alloy-mixing furnace for the fabrication of ingot. The alloy-mixing furnace temperature was kept 100 °C greater than the melting point of the compound for 2 days (48 h), during which the tube was continuously rotated and rocked at 10 rpm for uniform mixing and reaction. After that, the ingot was slowly cooled to room temperature (30 °C) over a period of 1 day (24 h). $\text{In}_2\text{Se}_{2.7}\text{Sb}_{0.3}$ single crystals were grown by Bridgman technique. The growth velocity and temperature gradient were 0.35 cm/h and 600 °C/cm respectively.

Using optical microscope, some interesting surface features were observed on the top free surface of the as-grown crystal which reveals the growth mechanism of the crystals. The as-grown crystal of $\text{In}_2\text{Se}_{2.7}\text{Sb}_{0.3}$ was viewed under contact mode. AFM was used to obtain a topographic image of the surface. Hall effect measurement was done with help of Ecopia Hall Effect measurement system (HMS-3000). The resistivity measurement was carried out at different temperatures in the range of 303 K to 393 K. For the E_g (band gap) study, a

*physicsathgce@gmail.com

†s_m_vyas_msu@yahoo.com

UV-Vis spectrophotometer was used for absorption data in the range of 200-900 nm.

3. RESULTS AND DISCUSSION

Numerous steps are revealed on the {110} faces, as can be seen in Fig. 1a. The step height is not extremely low, so probably these steps are formed due to bunching of lower steps. The formation of such macrosteps can only be understood if the {110} crystal face grows via a step-flow mechanism. From a periodic bond chain (PBC) [6, 7] analysis of several alums carried out by Encvort [8], it was found that {110} potash alum is an *F*-face since its growing layer contains two interconnected PCBs ($\bar{1}10$) and (001). Because, according to Harman in his research paper in 1980, in the morphological PCB theory on an *F*-face, the steps always run parallel to PBCs [9], it is to be expected that the step orientations on {110} crystal layer are parallel to the two directions ($\bar{1}10$) and (001). As the core of PBC ($\bar{1}10$) contains only the strong bonds and the core of PBC (001) contains also weaker interactions, it can be concluded that the PBC ($\bar{1}10$) is stronger than the PBC (001).

A further interesting phenomenon observed on numerous octahedral facets is the occurrence of reentrant corners in the step pattern. These are mainly found in the region between two grown hillocks as can be seen in phase contrast (Fig. 1b). From this figure, it can be gathered that the step with a reentrant corner has a slightly increased advancement rate. A similar effect, which can be deduced from the dependence of the step advancement rate in the step curvature derived by Burton, Cabrera and Frank, was observed for {111} potash alum and ADP and KDP single crystal. However, in contrast to potash alum, here the step orientations near the reentrant corner only slightly change and the “leg” of the V-shaped patterns maintains roughly parallel to the (110) direction so the conclusion, made from computer simulations that the shapes of the reentrant corner in a step are stable in time, also holds for the anisotropic crystal.

Energy dispersion spectra taken from the representative samples are shown in Fig. 2a. From this, we observe that wt. % of the elements are nearly the same. It shows that the grown crystals are nearly stoichiometric.

Fig. 2b shows 3D images of the crystal surface confirming the regular arrangement of atoms throughout the scanned region of the $\text{In}_2\text{Se}_{2.7}\text{Sb}_{0.3}$ single crystal. The morphology shows homogeneous distribution of small hill-like structures all over the as-grown crystal surface [5]. This uniform surface roughness suggests that the crystal growth is by layer mechanism. The layer growth mechanism is 2D lateral spreading of atoms [5, 6].

From the Hall effect measurements, the average Hall coefficient, resistivity, conductivity, mobility and carrier concentration of $\text{In}_2\text{Se}_{2.7}\text{Sb}_{0.3}$ single crystals are $-1.09 \times 10^7 \text{ Cm}^3/\text{C}$, $10.85 \times 10^4 \text{ }\Omega\text{-cm}$, $9.22 \times 10^{-6} \text{ 1}/\Omega\text{-cm}$, $248.85 \text{ Cm}^2/\text{Vs}$ and $2.31 \times 10^{11} \text{ 1}/\text{Cm}^3$, respectively. Resistivity data has good agreement with reported data for the single crystal [4]. The Hall coefficient was found to be negative indicating that the majority charge carriers are electrons and thus the material is *n*-type semiconductor. We also used hot probe methods to confirm $\text{In}_2\text{Se}_{2.7}\text{Sb}_{0.3}$ single crystal was found to be *n*-type.

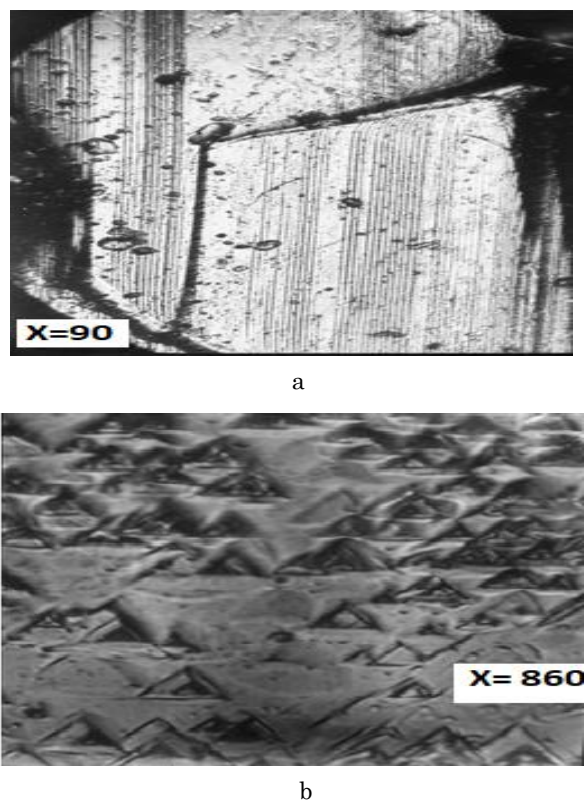


Fig. 1 – Growth features: (a) step strain on the crystal consisting of somewhat higher parallel steps; (b) reentrant corners in step pattern groups of hillocks and lower ($\sim 20 \text{ \AA}$) steps

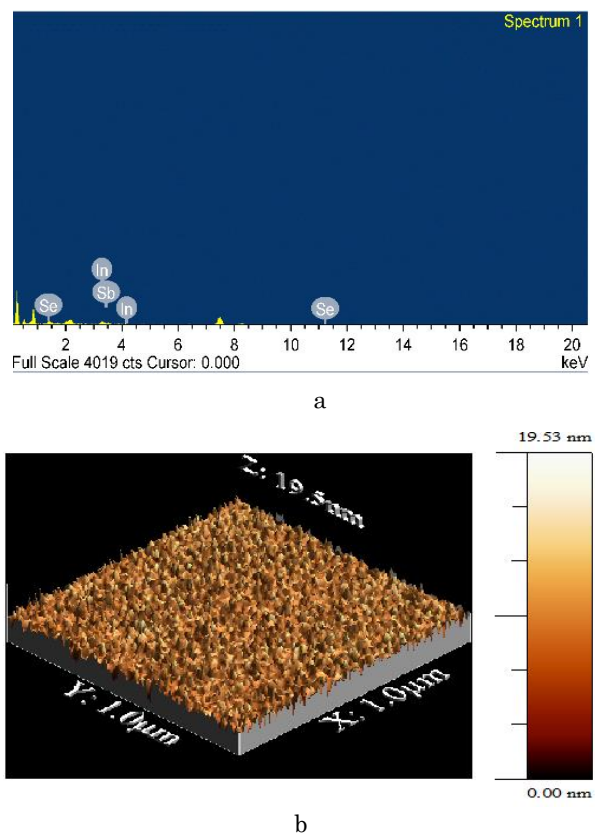


Fig. 2 – (a) EDAX spectra of energy v/s counts; (b) 3D AFM image of the $\text{In}_2\text{Se}_{2.7}\text{Sb}_{0.3}$ single crystal

The formula used to determine the resistivity is $\rho_0 = 2\pi SV/I$, where S is the probe separation distance, ρ is the resistivity. The four-probe measurement was carried out at different temperatures in the range of 303 K to 393 K. The room temperature resistivity value of $\text{In}_2\text{Se}_{2.7}\text{Sb}_{0.3}$ single crystal is $11.48 \times 10^4 \Omega\text{-cm}$.

The resistivity as a function of temperature is shown in the plot of $\ln(\rho(1/T))$ in Fig. 3.

The activation energy is obtained from the plot and given by the relation $\rho = \rho_0 \exp(-E_p/kT)$, where ρ is the resistivity, ρ_0 is the resistivity at room temperature, E_p is the activation energy equal to 0.4203 eV. The obtained values of electrical resistivity and activation energy are in good agreement with the value reported by various researchers [4].

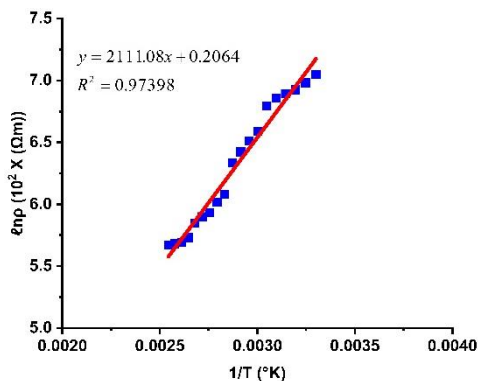


Fig. 3 – Resistivity plot

Absorption spectrum thus obtained follows the simple relationship between transmission and absorption, $A = -\log_{10}(T)$, where A is the absorption and T is the transmission. From the absorption data, Sharma et al. [7] have calculated the absorption coefficient (α) using the relation $\alpha = 2.303A/t$, where t is the thickness of crystal. The fundamental absorption, which corresponds to the transition from the valence band to the conduction band, can be used to determine the optical gap of the material.

Also, Dholakia et al. [8] wrote the relation between the absorption coefficient (α) and the incident photon energy ($h\nu$), $(\alpha h\nu) = B(h\nu - E_g)^r$, where B is a constant, E_g is the optical band gap of the material, r is the exponent which depends on the type of transition. r may have values of 1/2, 2, 3/2 and 3 corresponding to the allowed direct, allowed indirect, forbidden direct and forbidden indirect transitions, respectively. As using the value of exponent r , the exact values of optical band gap are calculated by extrapolating the straight-line

REFERENCES

1. J. Jasinski, W. Swider, J. Washburn, Z. Liliental-Weber, A. Chaiken, G.A. Gibson, C.C. Yang, *Lawrence Berkeley National Laboratory* **56**, 43 (2002).
2. H.M. Oh, H. Park, C.D. Kim, Y.S. Kim, K. Jang, W.T. Kim, *J. Korean Phys. Soc.* **43**, 20 (2003).
3. V.W.J.P. Bolt, R.J. Enckevort, *J. Cryst. Growth* **119**, 329 (1992).
4. W.J.P. Van Enckevort, R.J. Van Rosmalen, W.H. Van Der Linden, *J. Cryst. Growth* **49**, 502 (1980).
5. M.P. Deshpande, Nilesh N. Pandya, M.N. Parmar, *Turk. J. Phys.* **33**, 139 (2009).
6. Yoshinobu Kamakura, Nobuhiko Hosono, Aya Terashima, Susumu Kitagawa, Hirofumi Yoshikawa, Daisuke Tanaka, *Chem. Phys. Chem.* **19** No 17, 2134 (2018).
7. J. Sharma, G. Singh, A. Thakur, G.S.S. Saini, N. Goyal, S.K. Tripathi, *J. Opt. Elect. Adv. Mater.* **7**, 2085 (2005).
8. D.A. Dholakia, G.K. Solanki, S.G. Patel, M.K. Agarwal, *Scientia Iranica* **10** No 4, 373 (2003).

portion of $(\alpha h\nu)^{-1/r}$ vs. $h\nu$ plot to the $h\nu$ axis. Now for the direct band gap, the value of r is 1/2. Hence the direct band gap is obtained from the plot $(\alpha h\nu)^{-2}$ vs. $h\nu$ as shown in Fig. 4. The obtained value of direct band gap is 1.25 eV. Good agreement has been observed in the band gap values with earlier reports [4].

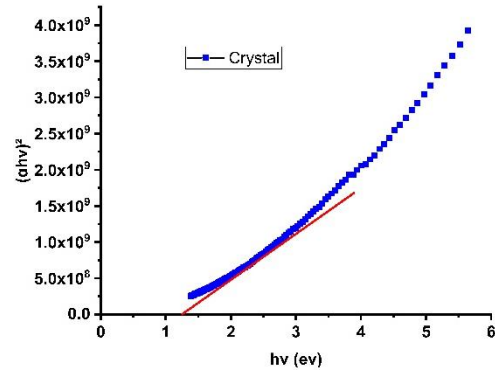


Fig. 4 – Plot of $(\alpha h\nu)^2$ v/s photon energy ($h\nu$)

4. CONCLUSIONS

The formation of such macrosteps can only be understood when the {110} face of crystals grows by the step flow mechanism. Also, it has been found that V-shaped patterns maintain roughly parallel to the (110) direction so that the shapes of the reentrant corner are stable in time that also holds for anisotropic crystal.

The as-grown single crystals have been found to possess nearly perfect stoichiometry by EDAX analysis.

The AFM image of the as-grown $\text{In}_2\text{Se}_{2.7}\text{Sb}_{0.3}$ single crystals shows a homogeneous distribution of small hill-like structures. This uniform surface roughness suggests that crystal growth by layer mechanism is predominant.

The optical allowed direct band gap of $\text{In}_2\text{Se}_{2.7}\text{Sb}_{0.3}$ single crystal was found to be 1.25 eV that is in agreement with the reported optical band gap of the material.

The Hall coefficient was found to be such that the material is an n -type semiconductor. The resistivity of $\text{In}_2\text{Se}_{2.7}\text{Sb}_{0.3}$ single crystal is found to be $11.48 \times 10^4 \Omega\text{-cm}$.

ACKNOWLEDGEMENTS

We are thankful to DRS-SAP and DST-FIST program sponsored to the Department of Physics school of science, Gujarat University, Ahmedabad, Gujarat, India. Authors are also thankful to Dr. P.R. Vyas and Prof. P.N. Gajjar, Head of physics department, school of sciences, Gujarat University, Ahmedabad for his constant encouragement.

Вирощування кристалів та електрооптичні характеристики сполуки $\text{In}_2\text{Se}_{2.7}\text{Sb}_{0.3}$ Piyush Patel¹, S.M. Vyas², Vimal Patel², Himanshu Pavagadhi²¹ *Department of Physics, Khyati Institute of Science, Khyati Foundation, Gujarat, India*² *Department of Physics, School of Sciences, Gujarat University, Ahmedabad, 380009 Gujarat, India*

III-VI групи напівпровідних матеріалів в основному використовуються для розробки детекторів іонізуючого випромінювання, твердотільних електродів, а також сонячних комірок, світлочутливих гетероструктур та іонних батарей. Шарова структура напівпровідникових кристалів III-VI групи була ретельно вивчена як двовимірна кристалічна система. Напівпровідник In_2Se_3 із загальною формулою сполуки A_2B_3 має гексагональну кристалічну структуру. Сполуку $\text{In}_2\text{Se}_{2.7}\text{Sb}_{0.3}$ вирощували за допомогою техніки Бріджмана. Температурний градієнт замерзання становив $60^\circ\text{C}/\text{см}$, і кристали найкращої якості були отримані зі швидкістю росту $0,35\text{ см}/\text{год}$. Досконалість кристала вивчалася під оптичним мікроскопом, з різною ознакою росту, який спостерігається на верхній вільній поверхні кристала, що є переважаючим механізмом росту шару. Для перевірки наявності складових елементів сполуки $\text{In}_2\text{Se}_{2.7}\text{Sb}_{0.3}$ використовувалася методика EDAX. Утворення дефектів в кристалах робить можливим зростання в умовах, близьких до рівноваги. У роботі атомно-силовою мікроскопією проведено морфологічне дослідження поверхні кристалічної сполуки. Використовуючи чотиризондову методику досліджено температурну залежність електричного питомого опору сполуки $\text{In}_2\text{Se}_{2.7}\text{Sb}_{0.3}$. Ширину забороненої зони визначали за допомогою UV-Vis спектрофотометра у діапазоні довжин хвиль від 200 нм до 900 нм . Результати та висновки з цих характеристик повідомляються в даній статті.

Ключові слова: Особливості поверхні, Ріст шару, Техніка Бріджмана, Питомий опір, Оптична ширина забороненої зони.